nature water

Article

https://doi.org/10.1038/s44221-024-00226-5

Walking-induced electrostatic charges enable in situ electroporated disinfection in portable water bottles

Received: 3 October 2023

Accepted: 7 March 2024

Published online: 12 April 2024

Check for updates

Young-Jun Kim[1,2,10], Zheng-Yang Huo[3,10] ✉, Xiaoxiong Wang[4,5,10], Haojie Dai[3], Dong-Min Lee[2,6], In-Yong Suh[1,2], Joon-Ha Hwang[1,7], Youngwook Chung[1,7], Hyeon Yeong Lee[1,2], Ye Du[8], Wenbo Ding[9] & Sang-Woo Kim[2,6] ✉

Direct in situ disinfection in portable water bottles could serve as the last line of defence for ensuring safe drinking water, especially in rural and disaster-stricken areas. However, limited disinfection technologies are available for this decentralized application due to the requirements of chemical inputs, a reliable energy supply and/or complicated modular constructions. Here we realized efficient in situ disinfection in a portable water bottle by directly harvesting the electrostatic charges induced by walking to stimulate electroporation. We fabricated a flexible non-metallic polypyrrole electrode with densely and uniformly distributed nanorods through nanopatterning and pasted it into a compact water bottle. Walking-induced electrostatic charges on the body surface can flow through a low-resistance path and accumulate on the nanorod tips to enhance local electric fields. These accumulated charges are sufficient to stimulate electroporation to realize the complete disinfection (>99.9999% inactivation) of a broad spectrum of microorganisms in a 500-ml water bottle within 10 minutes of walking.

Drinking water is a primary vector for the transmission of waterborne pathogens[1,2]. Ingesting pathogenic microorganisms in daily drinking water can lead to severe diseases[3,4]. Notably, waterborne pathogens can contaminate tap water even after centralized water treatment because microorganisms can regrow during subsequent storage and piped distribution[5]. In addition, rural, isolated or disaster-stricken areas that lack sanitation facilities urgently need to disinfect water before drinking[6,7]. Therefore, the direct in situ disinfection of water in portable containers is essential as a last line of defence to ensure water safety[8].

Conventional water disinfection methods, such as chlorination, ultraviolet irradiation and membrane filtration, can be used for decentralized microbial inactivation. However, their application in portable containers, such as water bottles, may be limited by additional chemical inputs (for example, chlorination tablets), the need for a stable power supply and decreased disinfection performance during long-term operation due to membrane fouling[9–12]. Emerging decentralized disinfection methods are primarily based on the generation of antimicrobial reactive oxidizing species (ROS) through electro- and photocatalytic

[1]School of Advanced Materials Science and Engineering, Sungkyunkwan University (SKKU), Suwon, Republic of Korea. [2]Center for Human-Oriented Triboelectric Energy Harvesting, Yonsei University, Seoul, Republic of Korea. [3]School of Environment and Natural Resources, Renmin University of China, Beijing, People's Republic of China. [4]Institute for Ocean Engineering, Tsinghua Shenzhen International Graduate School, Tsinghua University, Shenzhen, People's Republic of China. [5]Center of Double Helix, Tsinghua Shenzhen International Graduate School, Tsinghua University, Shenzhen, People's Republic of China. [6]Department of Materials Science and Engineering, Yonsei University, Seoul, Republic of Korea. [7]Research and Development Center, Energymining, Suwon, Republic of Korea. [8]College of Architecture and Environment, Sichuan University, Chengdu, People's Republic of China. [9]Tsinghua-Berkeley Shenzhen Institute, Tsinghua Shenzhen International Graduate School, Tsinghua University, Shenzhen, People's Republic of China. [10]These authors contributed equally: Young-Jun Kim, Zheng-Yang Huo, Xiaoxiong Wang. ✉e-mail: zhengyanghuo.edu@ruc.edu.cn; kimsw1@yonsei.ac.kr

methods[13–15]. However, these methods are strongly dependent on a stable supply of solar and/or electrical energy. In particular, the energy consumption of the electrocatalytic and photocatalytic methods range from 10^{-4} to 10^{0} kWh m^{-3} and 10^{-3} to 10^{6} kWh m^{-3}, respectively, for decentralized disinfection[16]. Recent studies have focused on generating ROS by harvesting ambient energy through tribo-, piezo-, thermo- and pyrocatalytic methods to overcome the restriction of a stable power supply[17–19]. Although these methods are feasible for some specific scenarios (for example, air conditioning with periodic temperature changes), their broader application is still hindered by fluctuating weather conditions and high thresholds of external stimuli. In addition, ROS can also oxidize the ubiquitous chloride ions in water to form active chlorine species, leading to the formation of harmful chlorinated disinfection by-products[20].

The development of a reaction-free physics-based disinfection technology that requires a tiny energy input could be a feasible alternative to realize in situ disinfection in portable water containers. Electroporation is an emerging physics-based method that relies on a strong electric field to compromise the outer structures of microorganisms (that is, bacterial membranes and viral capsids) for microbial inactivation[19,20]. The external voltage can be significantly reduced by using one-dimensional (1D) nanowires and nanorods with high aspect ratios to accumulate free charges and form highly localized electric fields at their tips[21–24]. Therefore, 1D nanomaterial-assisted electroporation can achieve complete microbial inactivation with an extremely low energy consumption ranging from 10^{-6} to 10^{-2} kWh m^{-3} (refs. 16,23–25). However, 1D nanomaterials, such as Ag, ZnO and Cu_3P, generally contain metallic material, which may raise concerns about the release of harmful metal ions into the drinking water[26–29]. In addition, it is difficult to realize electroporation with non-metallic carbon-based nanomaterials due to the weak adhesion of 1D nanostructures to the electrode[21].

Contact electrification is a common phenomenon that occurs whenever two materials with different dielectric properties come into contact[30–32]. In particular, electrostatic charges are easily generated on the body surface through contact electrification during daily human activities, such as walking, but their power density is relatively low[33]. Very recently, Kang et al. harvested walking-induced electrostatic charges for the first time to repulse negatively charged airborne particles[34]. This work demonstrated the potential of collecting body charges to drive a physics-based, energy-efficient process. Thus, although the energy density of the electrostatic charges on the body surface is relatively low, it might be sufficient to stimulate in situ electroporation disinfection in water bottles, which requires a tiny energy input.

Here we present a walking-electrification-induced electroporated disinfection (WEED) method for the in situ inactivation of bacteria and viruses in a portable water bottle. We incorporated a nanorod-modified polypyrrole (PPy) electrode fabricated by nanopatterning into a water bottle to accumulate charges at the nanorod tips to enhance the local electric field. The electrostatic charges harvested directly from the body surface have sufficient power density to induce physics-based electroporation to disinfect water. Over 99.9999% (6.0 log) of bacteria and viruses were inactivated in the water bottle (500 ml) in less than 10 min of walking. The WEED bottle exhibited high disinfection stability (80 cycle operation) with negligible material release, thereby ensuring a stable supply of safe drinking water.

Concept of the WEED method

The aim of this work was to use walking-induced electrostatic charges to drive electroporation disinfection in a portable water bottle (Fig. 1). The WEED method developed here involves a three-step process (Fig. 1a). Step 1: triboelectric charges are generated on shoes through contact electrification during walking. Step 2: the triboelectric charges accumulated on the shoes induce opposite electrostatic charges on the body surface through electrostatic induction. Step 3: the induced electrostatic charges flow through a low-resistance path and are collected on aluminium foil that is in contact with the hand and taped to the outer surface of the handheld disinfection bottle. The electrostatic body charges collected on the aluminium foil are transferred to the nanorod-modified electrode inside the bottle through a wire (Fig. 1b, left). The charges accumulate around the nanorod tips because they tend to migrate to the area of the electrode surface with the smallest radius of curvature. The accumulated charges induce an enhanced local electric field in the area of the nanorod tips to stimulate efficient microbial inactivation by electroporation when microorganisms (including bacteria and viruses) approach (Fig. 1b, right).

We prepared a metal-free, nanorod-modified PPy electrode to eliminate metal release into water using an easy-to-use nanopatterning fabrication method[35,36]. Nanopatterning is a commercial process for the scalable fabrication of carbon-based electrodes (up to several square metres). In brief, a poly(methyl methacrylate) (PMMA) film (200 μm) was first spin-coated onto a commercial nickel nanoimprint mould (20 cm × 20 cm) featuring a periodic nanorod structure to obtain a soft template with the negative image of the original nickel mould[31]. After sputtering indium tin oxide (ITO) onto the PMMA template surface, PPy was deposited onto the ITO/PMMA template via an electropolymerization process and easily separated from the ITO surface as a result of the significant difference in the surface energies of PPy and ITO (Supplementary Fig. 1)[35].

Thus, by using this scalable nanopatterning-assisted fabrication process, we fabricated a nanorod-modified PPy electrode with a large area of 225 cm^2 (15 cm × 15 cm; Fig. 1c, left). This metal-free, scalable electrode is 4.5 times larger than the largest metallic 1D nanomaterial-modified electrode (Cu_3P nanowire-modified copper mesh) currently used for electroporation disinfection[25]. The PPy nanorods accurately copy the periodic nanorod structure of the original nanoimprint mould with uniform lengths (~400 nm) and diameters (~50 nm; Fig. 1c, right) oriented perpendicular to the surface of the electrode (Fig. 1d,e). Owing to the strong covalent bonds, the polymerized PPy nanorods are more stable towards water treatment than metallic 1D nanomaterials with metallic or electrovalent bonds, preventing the release of material. The PPy nanorods exhibited high conductivity (~10^5 S cm^{-1}), confirming the feasibility of charge accumulation to provide enhanced local electric fields for electroporation (Supplementary Fig. 2). The surface potential (which corresponds to the local charge density) of the nanorods was evaluated by Kelvin probe force microscopy (KPFM), which revealed that the nanorods accumulate free charges at the tips (Fig. 1e,f). The simulated charge distribution on the nanorod surface (>6×10^4 C m^{-3}) and the corresponding enhanced local electric field (>10^7 V m^{-1}) further confirmed the high local charge enhancement (Fig. 1g and Supplementary Fig. 3).

Electrical output and disinfection performance

The walking-induced electrostatic charges were measured using a low-resistance handheld electrode connected to electrometer 1 (Fig. 2a, Extended Data Fig. 1a and Supplementary Video 1). The electrostatic body charges transferred to the handheld electrode achieved a high electrical output with an open-circuit peak-to-peak voltage of 304 V and a short-circuit peak-to-peak current of 17 μA at a fixed step rate of 0.5 Hz (Extended Data Fig. 1b). Increasing the step rate further enhanced the electrical output. Peak-to-peak voltages of 341, 405 and 493 V were generated at step rates of 1, 1.5 and 2 Hz, respectively (Fig. 2b and Extended Data Fig. 1c). The electrical output generally improved as the triboelectric charge density of the shoe material increased[33]. Leather, with a relatively low triboelectric charge density (53 μC m^{-2}), exhibited a limited output voltage (96 V), while polycarbonate (PC), rubber and poly(vinyl chloride) (PVC), with triboelectric charge densities greater than 105 μC m^{-2}, generated output voltages of >250 V (Fig. 2c)[37]. Similarly, materials with higher triboelectric charge densities generated higher output currents during walking (Fig. 2c).

https://doi.org/10.1038/s44221-024-00226-5

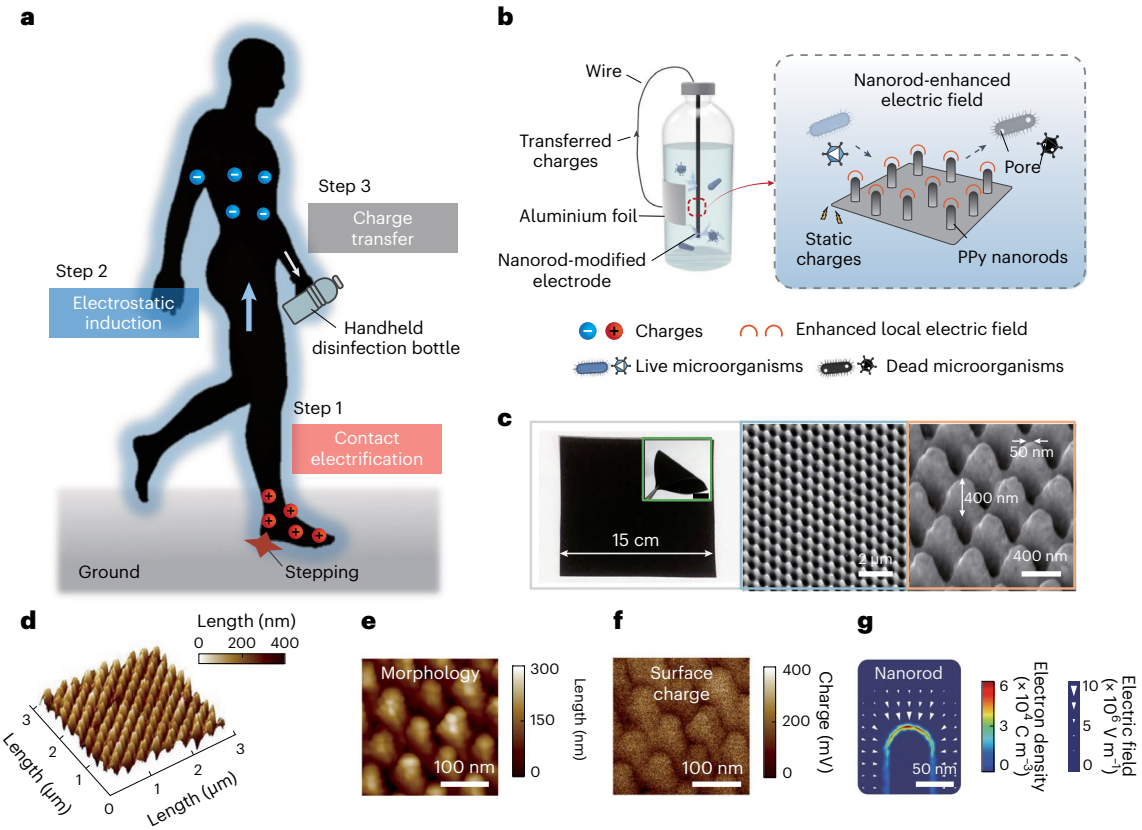

Fig. 1 | Concept of the WEED method. a, Working principle of the WEED method. Step 1: triboelectric charges are generated on shoes through contact electrification during walking. Step 2: The triboelectric charges accumulated on the shoes induce opposite electrostatic charges on the body surface through electrostatic induction. Step 3: The induced electrostatic charges transfer through a low-resistance path and accumulate on aluminium foil taped to the bottle surface that is in contact with the hand. **b**, Schematic illustrating the construction of the handheld WEED bottle and the microbial inactivation mechanism. **c**, Photograph (left) and high-resolution SEM images (middle and right) of the nanorod-modified PPy electrode. Inset: photograph of the folded electrode (scale bar, 5 mm). **d**, AFM image showing the surface morphology of the nanorod-modified PPy electrode. **e**, High-resolution AFM image showing the surface morphology of the PPy nanorods. **f**, KPFM image showing the corresponding surface charge of the PPy nanorods. **g**, Simulated electron density (colour map) and electric field close to the PPy nanorod, illustrating the accumulated charges and corresponding enhanced local electric field.

The triboelectric charges generated at the shoe–ground interface were measured using electrometer 2 and compared with those transferred to the hand, measured by electrometer 1 (Fig. 2a), to evaluate the efficiency of the electrostatic charge transfer during walking (Fig. 2d). Higher triboelectric charge densities resulted in increased transfer efficiencies. Over 70% of the triboelectric charges generated at the shoe–ground interface were transferred to the handheld electrode when wearing shoes made of PC, rubber or PVC. In comparison, only 32% of the charges were transferred to the hand when wearing leather shoes (Fig. 2d). The difference in the transfer efficiency of the electrostatic body charges for the different footwear materials indicates that a large proportion of the triboelectric charges generated at the shoe–ground interface can overcome body resistance (Fig. 2d)[38]. In addition, when wearing PVC shoes for walking at a fixed step rate of 1 Hz, a maximum power density of 70 mW m^{-2} was achieved (Extended Data Fig. 1d). Increasing the step rate to 2 Hz further improved the power output (Extended Data Fig. 1e). Therefore, the walking-induced electrostatic charges are readily available for power generation when a person walks on the ground.

We confirmed the feasibility of the WEED method for water disinfection using a laboratory-scale disinfection demonstrator (5 cm long with a cross-sectional area of 2.5 cm^2; Fig. 2e). Systematic evaluation and optimization of the WEED method in the laboratory-scale disinfection demonstrator could ensure that the proposed method is ready for incorporation into portable bottles. Two model bacteria species (Gram-negative *Escherichia coli* and Gram-positive *Bacillus subtilis* (*B. subtilis*)) and a model virus species (MS2, an *E. coli* bacteriophage), as an indicator for human enteric viruses, were used in the disinfection demonstrator to evaluate its performance. High concentrations of bacteria (10^6 colony-forming units per ml (CFU ml^{-1})) or viruses (10^6 plaque-forming units per ml (PFU ml^{-1})) were added to 10 mM phosphate-buffered saline (PBS) solution to simulate tap or surface water with the necessary conductivity and pH-buffering capacity. We used log removal efficiency ($-\log(C/C_0)$) to quantify the disinfection performance, considering the high demand for realizing near-complete disinfection of water containing high concentrations of bacteria[39–41]. Water samples containing microorganisms flowed through the system at a targeted flow rate (1–10 ml min^{-1}) to simulate the specific residence time (that is, operating time) in the water bottle. The nanorod-modified PPy electrode was taped to the inner surface of the demonstrator, which was connected to a handheld electrode to collect the electrostatic body charges generated during walking for water disinfection (Fig. 2e).

The WEED demonstrator achieved complete disinfection of *E. coli* (6.0 log removal, that is, >99.9999% inactivation) with a fixed step rate of 1 Hz at flow rates of 1, 3 and 5 ml min^{-1}, corresponding to residence times in the water bottle of 5, 1.6 and 1 min, respectively (Fig. 2f). Increasing the flow rate to 10 ml min^{-1} resulted in a shortened residence time of 30 s, which slightly affected the disinfection efficiency (5.2 log *E. coli* removal, corresponding to >99.999% inactivation). Similarly, the

https://doi.org/10.1038/s44221-024-00226-5

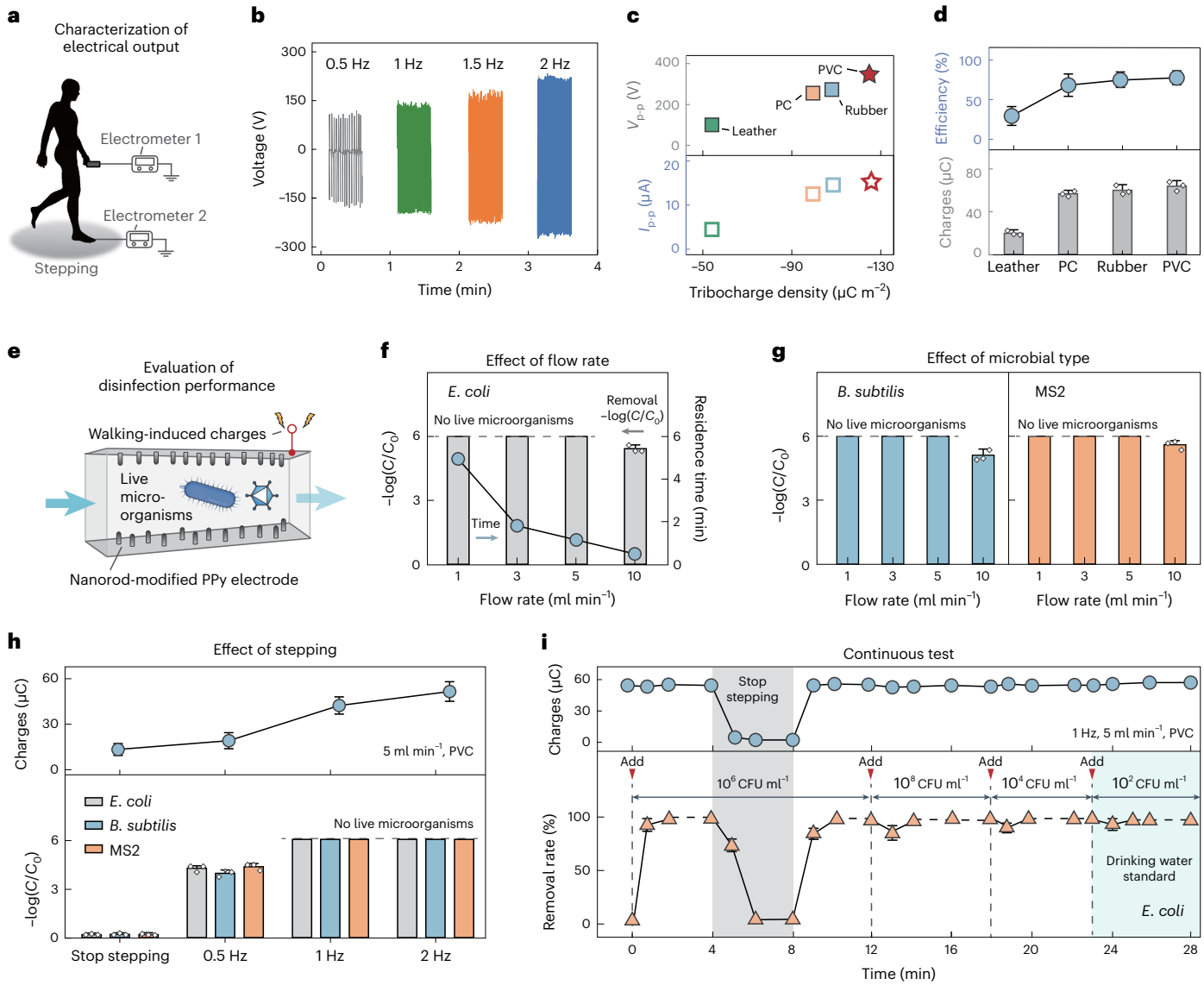

Fig. 2 | Electrical output and disinfection performance of the WEED method. **a**, Schematic illustrating the set-up for electrical output measurement using handheld electrodes. **b**, Electrical output at various step rates (0.5–2 Hz). **c**, Effect of footwear material with different triboelectric charge density on the peak-to-peak voltage ($V_{p\text{-}p}$; top) and current ($I_{p\text{-}p}$; bottom). **d**, Effect of footwear material on charge generation (bottom) and the corresponding charge transfer efficiency (top) from foot to hand. **e**, Schematic illustrating the set-up for evaluating disinfection performance using a laboratory-scale WEED demonstrator. The nanorod-modified PPy electrodes are taped to the inner surface of the demonstrator, which is connected to a handheld electrode to collect the electrostatic charges generated during walking. **f**, Effect of flow rate (1–10 ml min^{-1}) and the corresponding residence time on the disinfection efficiency ($-\log(C/C_0)$) for *E. coli* (Gram-negative bacterium). **g**, Disinfection efficiency for different model microbes: *B. subtilis* (Gram-positive bacterium) and MS2 (bacteriophage virus). **h**, Effect of step rate on the charge generation efficiency (top) and disinfection performance (bottom). **i**, Walking-induced charge generation efficiency (top) and disinfection performance (bottom) with and without stepping (grey area) for inactivating different concentrations of *E. coli* (10^2–10^8 CFU ml^{-1}) under continuous operation. Experiments were conducted in a 10 mM PBS buffer at pH 7.0. The step rate was fixed at 1 Hz in **f**, **g** and **i**, and the flow rate was fixed at 5 ml min^{-1} in **h** and **i**. The dashed lines in **f**–**h** indicate that all of the microorganisms were inactivated (that is, no live microorganisms were detected). Error bars represent the standard deviation (s.d.; $n = 3$) and the data are presented as mean values ± s.d. in **d** and **f**–**i**.

WEED method enabled the complete disinfection of *B. subtilis* and MS2 at flow rates of 1–5 ml min^{-1} with reduced efficiency (<5.0 log removal) at the higher flow rate of 10 ml min^{-1} (Fig. 2g).

We further investigated the contribution of walking-induced electrostatic charges to microbial disinfection. Disinfection efficiency improved as the electrostatic body charges increased. At a step rate of 0.5 Hz, the WEED method harvested 14 nC of charge on the electrode and enabled >4.2 log microbial removal (>99.99% inactivation) at a fixed flow rate of 5 ml min^{-1}. Increasing the step rate to 1 and 2 Hz induced an increasing amount of electrostatic charge on the electrode (>42 nC), resulting in an improved disinfection efficiency (complete inactivation, >6.0 log removal) for all of the tested microorganisms (Fig. 2h). In addition, walking in shoes made with PC, rubber or PVC, which have high triboelectric charge densities (>105 μC m^{-2}), generated large amounts of electrostatic charge (>45 nC) and achieved complete water disinfection (>6.0 log removal; Supplementary Fig. 4)[37]. In contrast, shoes made of leather, with a lower triboelectric charge density (34 μC m^{-2}), generated limited electrostatic charge (27 nC) and attained a reduced disinfection efficiency (<3.0 log removal)[37].

https://doi.org/10.1038/s44221-024-00226-5

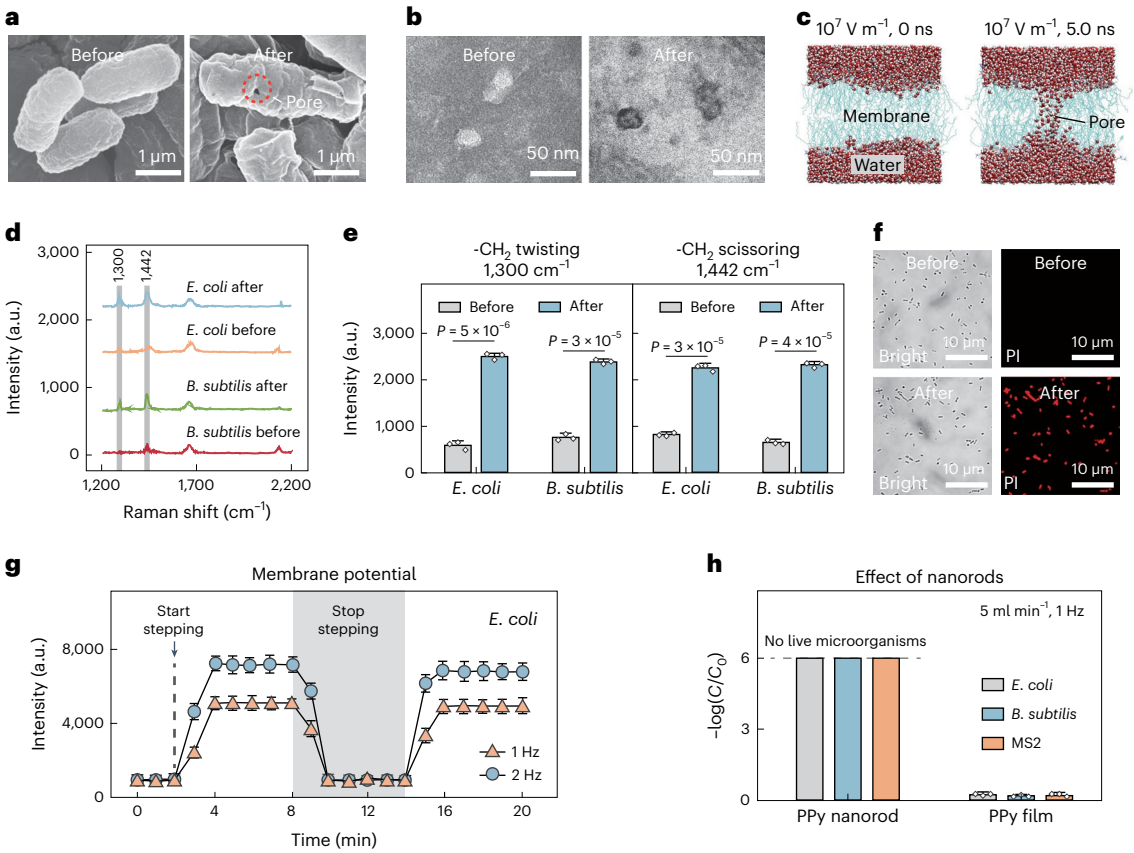

Fig. 3 | Investigation of the mechanism of the WEED process. a, SEM images of *E. coli* before and after WEED treatment. **b**, TEM images of MS2 before and after WEED treatment. **c**, MD simulations describing the bacterial membrane before (left) and after (right) electroporation under an enhanced electric field of 10^7 V m^{-1}. **d**, Raman spectra of *E. coli* and *B. subtilis* before and after WEED treatment, averaged over ten individual cells. **e**, Intensities of the -CH_2 twisting and scissoring readout from the Raman measurements. **f**, Bright-field (total bacteria) and fluorescence (inactivated bacteria) microscopy images of *E. coli* before and after WEED treatment. **g**, Evaluation of membrane potential with and without stepping during WEED operation. **h**, Disinfection efficiency of the WEED method using a nanorod-modified PPy electrode or a PPy film electrode. The experiments were conducted in the disinfection demonstrator in 10 mM PBS buffer at pH 7.0. The flow and step rates were fixed at 5 ml min^{-1} and 1 Hz, respectively. The dashed lines indicate that all of the microorganisms were inactivated (that is, no live microorganisms were detected). Error bars represent the s.d. ($n = 3$) and data are presented as mean values ± s.d. in **e**, **g** and **h**. One-way analysis of variance was performed using Tukey's post hoc test to analyse the significant differences ($P < 0.05$) between the groups in **e**.

We also performed a continuous disinfection test and observed that microbial inactivation was strongly dependent on the amount of walking-induced electrostatic charge (Fig. 2i). The WEED method achieved complete disinfection for all of the tested microorganisms within 2 min of walking (1 Hz). Stopping walking resulted in negligible electrostatic charge generation, which immediately reduced the disinfection efficiency. When walking resumed, complete disinfection was restored within 2 min. In addition, the WEED method achieved complete disinfection over a wide range of bacterial (10^2–10^8 CFU ml^{-1}) and viral (10^2–10^6 PFU ml^{-1}) concentrations (Fig. 2i and Supplementary Fig. 5). These results indicate not only the high disinfection capacity of the WEED method but also the feasibility of its application to treat water with microbial concentrations common in real situations.

Disinfection mechanisms of the WEED method

The electroporation disinfection mechanism was evaluated by analysing the microbial morphology using scanning electron microscopy (SEM; for bacteria) and transmission electron microscopy (TEM; for viruses). The bacteria (*E. coli* and *B. subtilis*) showed small pores (<100 nm) on the membrane surface without obvious collapse after WEED treatment, indicating that electroporation primarily contributes to the inactivation of bacteria (Fig. 3a and Supplementary Fig. 6). Negative stain-incorporated TEM is used to assess the integrity of viral capsids[25]. Viruses with damaged capsids can be stained with phosphotungstic acid, visualized as a dark contrast in TEM images. Indeed, the WEED-treated virus (MS2) exhibited such dark contrasts, indicating the perforation of the viral capsids by electroporation (Fig. 3b).

We further confirmed the disinfection of bacteria by electroporation in WEED treatment by investigating the structure of the bacterial membrane at the molecular level using molecular dynamics (MD) methods (Supplementary Fig. 7). The carbon chains of the phospholipid bilayer in the bacterial membranes exhibited a twisted structure in an electric field of 10^7 V m^{-1}, resulting in a small channel of water (that is, an electroporation pore) that penetrates the entire membrane within 5 ns (Fig. 3c)[42]. The electroporation-induced perforation of the membrane during WEED operation was further confirmed experimentally using Raman spectroscopy (Fig. 3d). The treated *E. coli* and *B. subtilis* exhibited higher intensities at 1,300 and 1,442 cm^{-1}, corresponding to enhanced twisting and scissoring, respectively, of the carbon chain (-CH_2) in the phospholipid bilayer of the membrane (Fig. 3e)[43]. The increased permeability of the membrane after WEED treatment was also evidenced by a staining test with propidium iodide (PI), a bacterial stain that can penetrate cells with damaged membranes, which is also indicative of the disinfection mechanism of electroporation[22]. Few cells showed compromised membrane structures before WEED treatment. In contrast, over 95% of the cells were stained (that is, showed red fluorescence) after treatment, indicating increased membrane

permeability due to electroporation (Fig. 3f and Extended Data Fig. 2a). Furthermore, the live/dead staining test also showed compromised bacterial membranes after WEED treatment (Supplementary Fig. 8).

We next evaluated the membrane potential of bacteria during WEED treatment because the compromised membrane structure may lead to unwanted and uncontrollable ion exchange across the cell membrane (that is, membrane depolarization), resulting in a fluctuation of the transmembrane voltage. The fluorescent probe 3,3′-dipropylthiadicarbocyanine iodide (DiSC3(5)) can be used to probe the structure of the test bacteria because it can accumulate in cell membranes while maintaining a fluorescence quenching state[44]. When the membrane potential disappears, DiSC3(5) is released into the surrounding substrate and subsequently generates fluorescence. During WEED treatment, DiSC3(5) fluorescence increased rapidly with generated electrostatic charges in a dose-dependent manner (that is, with step rate), indicating a significant change in the membrane potential. In contrast, when walking stopped, limited electrostatic charges were generated, as indicated by the negligible fluorescence intensity (Fig. 3g). We confirmed the negligible contribution of oxidative species (·OH and $O_2^{\cdot-}$) to disinfection by the addition of radical scavengers, which can quench any generated oxidative species to eliminate oxidation. In contrast to the previous experiment, which suggested that the disrupted membrane potential may be due to the generation of oxidative species during WEED treatment, the added radical scavengers (isopropanol for ·OH and benzoquinone for $O_2^{\cdot-}$) had no effect on the microbial disinfection, indicating negligible chemical oxidation (Extended Data Fig. 2b)[25].

We compared the disinfection efficacy of the nanorod-modified PPy electrode with that of a flat PPy film electrode to demonstrate the successful accumulation of walking-induced electrostatic charges at the tips, which provide enhanced electric fields for electroporation. The nanorod-modified electrode achieved complete microbial disinfection (>6.0 log), whereas the flat PPy film was ineffective (<0.2 log removal) under the same operating conditions (Fig. 3h). We have also demonstrated the negligible effects of intracellular oxidative stress (Extended Data Fig. 2c) and temperature fluctuation (Extended Data Fig. 2d) on WEED disinfection.

Water disinfection using a handheld WEED bottle

We designed a prototype WEED bottle based on the demonstrator. The WEED bottle consists of a poly(ethylene terephthalate) (PET) bottle, a piece of aluminium foil (2 cm × 2 cm), four parallel nanorod-modified PPy electrodes (each with an area of 4 cm × 15 cm) and a copper wire (Fig. 4a and Extended Data Fig. 3). When disinfection is required, a person can conveniently fill the PET bottle (~500 ml) with water and then hold it so that his or her hand is in contact with the aluminium foil. After walking for a short time (for example, several minutes), the microorganisms in the water are effectively inactivated for on-demand water disinfection.

The disinfection efficacy of the walking-induced disinfection bottle was evaluated by treating 500 ml of 10 mM PBS buffer solution dosed with high concentrations of bacteria or viruses (10^6 CFU ml^{-1} or 10^6 PFU ml^{-1}, respectively; Supplementary Video 2). All of the bacteria and viruses tested were completely inactivated with negligible live microorganisms detected in water after 10 min of walking at a fixed step rate of 1 Hz (Fig. 4b and Supplementary Fig. 9). Increasing the step rate improved the disinfection performance. A faster step rate of 2 Hz reduced the time required for complete disinfection from 12 min (step rate of 0.5 Hz) to 7 min (Supplementary Fig. 10). The treatment time was further reduced when running (~3 Hz; Supplementary Fig. 10). The operation time for complete disinfection increased to 13 min when treating a larger volume of water (1,000 ml) at a step rate of 2 Hz (Supplementary Fig. 11). Notably, the walking-induced disinfection bottle achieved complete disinfection (>6.0 log) for all of the tested microorganisms (*E. coli*, *B. subtilis* and MS2) dosed in tap, river and lake water when a person walked for 10 min at a step rate of 1 Hz while holding the 500-ml disinfection bottle (Fig. 4c) in a wide range of humidities from 20% to 90% (Supplementary Fig. 12). In addition, reducing the electrode spacing effectively improved the disinfection performance due to the increased electric field between the electrodes (Supplementary Fig. 13).

The feasibility of the walking-induced disinfection bottle was further confirmed by conducting a long-term test and evaluating the disinfection performance over a significant number of operating cycles. In each cycle, river water (500 ml) containing microorganisms (bacteria or viruses) was treated in the walking-induced disinfection bottle for 10 min at a fixed step rate of 1 Hz. The walking-induced disinfection bottle achieved complete disinfection (>6.0 log) for 80 continuous cycles with no live microorganisms detected in the water (Fig. 4d). Furthermore, the nanorod-modified PPy electrodes with a robust structure and inert chemical properties remained stable. Only slight morphological and compositional changes were observed in the electrodes with negligible release of pyrrole (not detected) and copper ions (<4 μg l^{-1}) into the water after 80 cycles of operation (Fig. 4d,e, Supplementary Fig. 14 and Supplementary Table 1). In addition, negligible organic fouling of the electrode surface was observed after long-term operation (Supplementary Fig. 14). These results demonstrate the feasibility of using the WEED bottle to treat river water with a relatively low concentration of organics (total organic carbon concentration <5 mg l^{-1}). Our proposed WEED bottle also enables the inactivation of both Gram-positive (*B. subtilis*) and Gram-negative bacteria (*E. coli*) as well as viruses (MS2) to meet real-world scenarios for in situ water disinfection (Fig. 4f–h and Supplementary Fig. 15).

Discussion

We have realized direct in situ disinfection of bacteria and viruses in a portable water bottle using walking-induced electrostatic charges to drive 1D nanomaterial-assisted electroporation. Walking-induced electrostatic charges can flow through a low-resistance path and accumulate on the tips of a nanorod-modified PPy electrode to enhance local electric fields. The flexible non-metallic PPy electrode with periodic nanorods can be easily pasted into the water bottle for in situ disinfection before drinking. Bacteria and viruses were completely inactivated (>99.9999% inactivation) in the 500-ml water bottle in a few minutes (<10 min) of walking. The WEED bottle also demonstrated high stability over 80 cycles (equivalent to 800 min of continuous operation) with negligible release of material during operation, ensuring a reliable supply of safe drinking water. The disinfection performance may be further improved by replacing the plate electrodes with porous flow-through electrodes to enhance the transfer of microbial cells. Increasing the surface area of the PPy electrode may also help to increase the disinfection efficiency.

Centralized water treatment is primarily used for municipal water disinfection. However, current technologies are unsuitable for direct disinfection in water bottles before drinking due to their reliance on multiple facilities with a stable power supply (Fig. 4i, top). In addition, waterborne pathogens can regrow during storage and piped distribution after centralized water treatment, threatening the safety of drinking water. In contrast, our proposed WEED treatment process, driven by walking-induced electrostatic charges, can achieve highly efficient disinfection in water bottles without relying on external power supplies (Fig. 4i, bottom). Furthermore, the use of the WEED method for direct disinfection in a water bottle can minimize the impact of microorganism regrowth, ideally serving as the last line of defence for safe drinking water. Moreover, the WEED bottle can easily realize in situ water disinfection to meet the urgent need for safe drinking in rural, isolated or disaster-stricken areas that lack sanitation facilities and a stable electricity supply at a low fabrication cost (<US$2 for a 500-ml WEED bottle; Supplementary Table 2). In summary, this study provides a viable approach to highly efficient, in situ water disinfection in portable containers (for example, bottles and cups) without the constraints

https://doi.org/10.1038/s44221-024-00226-5

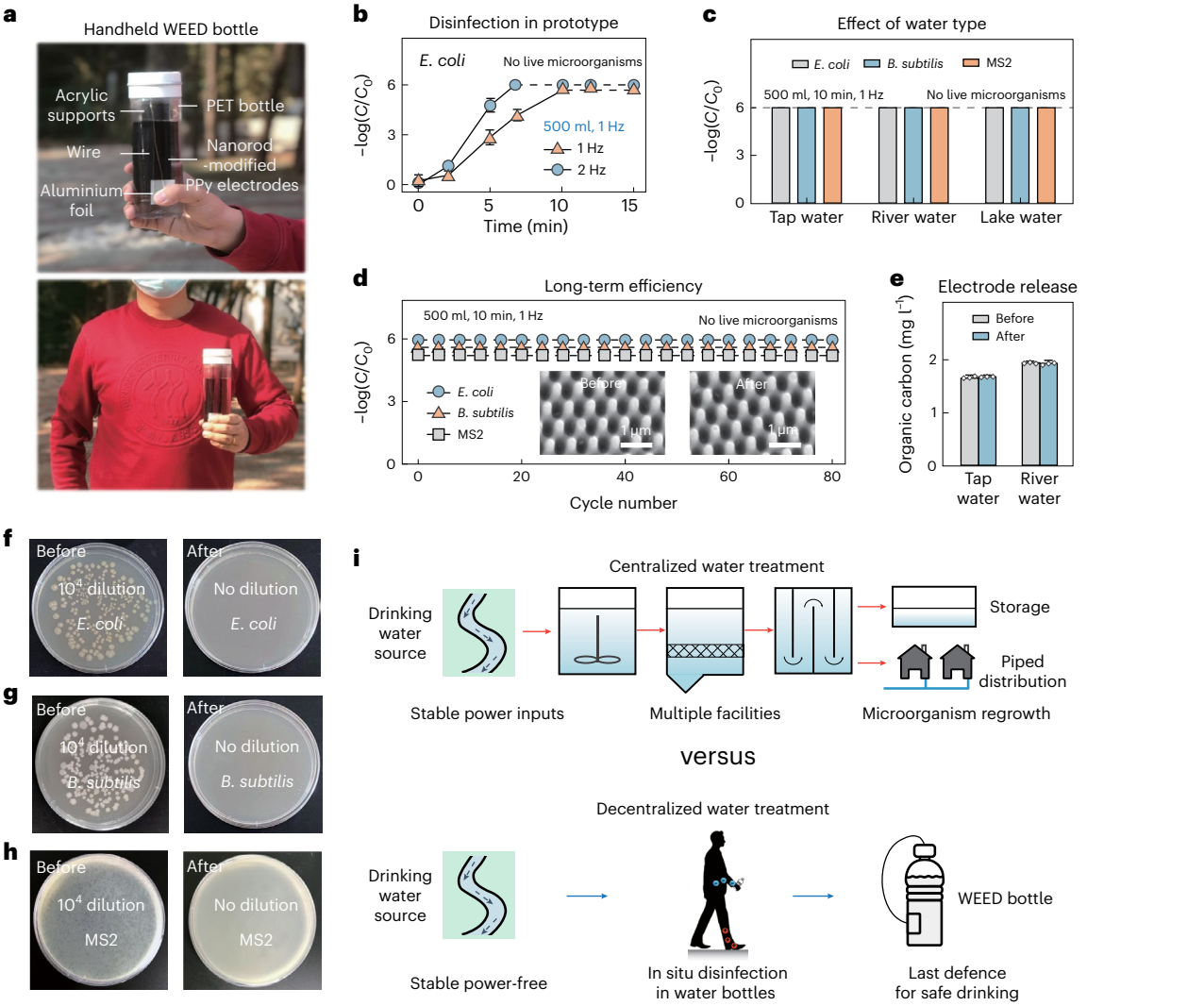

Fig. 4 | Disinfection performance of the handheld WEED bottle. **a**, Photographs of the handheld WEED bottle. **b**, Disinfection efficiency of the WEED bottle for treating 500 ml water containing 10^6 CFU ml^{-1} *E. coli*. **c**, Disinfection efficiency of the WEED bottle for treating different types of infected water. **d**, Long-term stability of the WEED bottle in disinfection tests. River water containing microorganisms was treated for 10 min in each cycle and a total of 80 cycles were performed. Insets: SEM images showing the morphology of the PPy nanorods before and after operation. **e**, Evaluation of electrode stability during long-term disinfection. Concentration of organic carbon in the tap and river water before and after continuous operation for 800 min without microorganism dosing. **f**–**h**, Plating photographs showing the concentration of *E. coli* (**f**), *B. subtilis* (**g**) and MS2 (**h**) before and after disinfection using the WEED bottle. **i**, Schematic illustrating the advantages of the decentralized WEED bottle over centralized water treatment. Conventional centralized treatment requires multiple facilities with continuous energy input on a large scale, while the portable WEED bottle can achieve in situ water disinfection before drinking without external power supplies. The dashed lines in **b**–**d** indicate that all of the microorganisms were inactivated (that is, no live microorganisms were detected). Error bars represent the s.d. ($n = 3$) and data are presented as mean values ± s.d. in **e**.

of a stable power supply and complicated modular constructions, ensuring the last line of defence of water safety.

Methods

Materials preparation

Methyl methacrylate (MMA) was dissolved in toluene with a target ratio of 8.3 MMA/toluene and spin-coated (500 r.p.m. for 30 s) onto the surface of a commercial nickel nanoimprint mould with high-performance antireflective nanorod structures (20 cm × 20 cm; HT-AR-02C, Temicon)[35]. After drying under vacuum at 60 °C, a 200-μm-thick PMMA film was fabricated with the negative image of the original nickel mould. After separating the PMMA film and nickel mould in water, the PMMA template was cut to a desired size (15 cm × 15 cm) and sputter-coated with ITO using a magnetron sputtering system (ATC Orion 5, AJA International). PPy was deposited onto the ITO/PMMA template by immersing the template in an electrolyte solution containing pyrrole (0.1 mol l^{-1}) and *p*-toluenesulfonic acid (0.2 mol l^{-1})[35] in an electropolymerization process. The prepared ITO/PMMA template and a carbon paper electrode were selected as the working and counter electrodes, respectively. A target current density of 0.1 mA cm^{-2} was applied using a potentiostat (Interface 1010E, Gamry). A flat PPy film electrode was prepared by a similar method using a flat ITO electrode as template. The morphologies of the prepared electrodes were characterized by SEM (JSM-6701F, JEOL) and atomic force microscopy (AFM) (XE-100, Park Systems).

Electrical characterization

The electrostatic body charges generated by walking were harnessed using an electrode. The electrode was attached to either the hands or shoes of a person (Extended Data Fig. 1a). The output voltage was

measured using an oscilloscope (DPO3052, Tektronix), and a low-noise current amplifier (DLPCA-200, FEMTO) was used to measure the output current[25]. The electrical output of the electrostatic charges was measured while wearing shoes made of different materials (leather, PC, rubber or PVC) and at step rates ranging from 0.5 to 2 Hz (Extended Data Fig. 3a). Typically, the experiments were conducted at a relative humidity of 65.0% and temperature of 20 °C.

Evaluation of the disinfection

E. coli (ATCC, 15597) and *B. subtilis* (ATCC, 23857) were cultured in trypticase soy broth at 37 °C for 12 h and then washed with deionized water by centrifugation (2,000*g*). Bacteriophage MS2 (ATCC, 15597-B1) was cultured by growing with *E. coli* at 37 °C for 2 h. A feed solution (10 mM PBS) containing bacteria (10^6 CFU ml^{-1}) or virus (10^6 PFU ml^{-1}) was used to evaluate the log disinfection efficiency (*E*) as follows:

$$E = -\log\left(\frac{C}{C_0}\right) \quad (1)$$

where C_0 and C are the concentrations of live microorganisms before and after the operation, respectively. The number of live bacteria and viruses was measured by the standard spread plating and double agar layer methods, respectively[25].

Device construction

A laboratory-scale disinfection demonstrator with a length of 5 cm and a cross-sectional area of 2.5 cm^2 was fabricated to investigate the disinfection performance. Four nanorod-modified PPy electrodes, each with a target area of 1.6 cm × 5 cm, were taped to the inner surface of the demonstrator and connected to the handheld electrode by a conductive wire. During the disinfection test, a person holding the device walked continuously at a fixed step rate of 0.5–2 Hz. A metronome was used to produce a precisely controlled sound to remind the operator to step at the desired frequency. A 10 mM PBS solution containing bacteria (*E. coli* or *B. subtilis*; 10^6 CFU ml^{-1}) or virus (MS2; 10^6 PFU ml^{-1}) was passed through the disinfection demonstrator at a targeted flow rate of 1–10 ml min^{-1}, controlled by a syringe pump.

A handheld walking-stimulated disinfection bottle was developed consisting of a 500-ml PET bottle, a piece of conductive aluminium foil (2 cm × 2 cm) on the outer surface of the bottle, two parallel acrylic supports (with an area of 4 cm × 15 cm and a gap of 2 cm between each support), and four nanorod-modified PPy electrodes (4 cm × 15 cm) attached to each acrylic support and connected to the aluminium foil by a conductive wire. Bacteria (*E. coli* and *B. subtilis*) and a virus (MS2) were dosed into 10 mM PBS solution, tap water, river water and lake water (detailed water quality parameters are presented in Supplementary Table 3) at the target concentrations of 10^6 CFU ml^{-1} and 10^6 PFU ml^{-1}, respectively. During disinfection, a person held the disinfection bottle containing 500 ml of the water sample dosed with microorganisms and ensured that his or her hand was in contact with the aluminium foil while he or she walked for a controlled time; the concentration of the microorganisms in the bottle before and after the operation was evaluated. The concentration of organic carbon in the effluents before and after the treatment of tap and river water for 80 cycles without dosing microorganisms was also measured using a trace total organic carbon analyser (TOC-L, Shimadzu).

Mechanistic investigation

The surface potential of the electrode was measured by KPFM (XE-100, Park Systems) with Cr/Au-coated silicon tips. The charge density and electric field strength were investigated using COMSOL Multiphysics software. A model comprising two electrodes (2 cm × 4 cm) with a gap of 0.5 mm between them was built. An array (6 × 6) of nanorods (length 400 nm and diameter 50 nm) was oriented perpendicular to the electrode surface. Charges of 60 μC were applied to the electrodes (see Supplementary Fig. 3 and Supplementary Table 4 for details).

The bacterial morphology was examined by SEM (JSM-6701F, JEOL). *E. coli* cells were collected by centrifugation (2,000*g*) and stored in 2% glutaraldehyde solution overnight at 4 °C. After dehydration with ethanol, the *E. coli* samples were freeze-dried[25]. The viral morphology was examined by TEM (JEM-2100F, JEOL). A sample of MS2 (~500 μl) was dropped onto a TEM copper grid and then stained with 1% phosphotungstic acid solution for TEM characterization[25].

Bacterial membranes in electric fields (10^7 V m^{-1}) were evaluated at the atomic level through MD simulations (see Supplementary Fig. 7 and Supplementary Table 5 for details of the procedure and parameters). The structure of the bacteria (*E. coli* and *B. subtilis*) was studied experimentally by single-cell Raman spectroscopy (Alpha300 Ri, WITec), with at least ten cells measured for each sample following excitation at 514 nm (ref. 43). Bacterial membrane permeability was assessed by fluorescence microscopy (ECLIPSE Ts2, Nikon). Bacterial samples were stained with 2 mM PI and observed by bright-field microscopy (whole bacteria) and fluorescence microscopy (535 nm, membrane-compromised bacteria)[28]. The bacterial membrane potential was evaluated using the DiSC3(5) staining assay, in which 0.5 μM DiSC3(5) was added to a feed solution containing *E. coli* (10^6 CFU ml^{-1}). After passing through the disinfection demonstrator, the stained cells were collected and measured using a microplate photometer (Multiskan FC, Thermo Scientific) with excitation and emission wavelengths of 622 and 670 nm, respectively[44].

Statistical analysis

Statistical analyses were performed using the Prism 9 software (9.5.0, GraphPad). One-way analysis of variance was performed using Tukey's post hoc test to analyse significant differences ($P < 0.05$).

Reporting summary

Further information on research design is available in the Nature Portfolio Reporting Summary linked to this article.

Data availability

The data supporting the findings of this study are available within this paper and the Supplementary Information. Other relevant data are available from the corresponding authors upon reasonable request. Source data are provided with this paper.

References

1. Wolf, J. et al. Effectiveness of interventions to improve drinking water, sanitation, and handwashing with soap on risk of diarrhoeal disease in children in low-income and middle-income settings: a systematic review and meta-analysis. *Lancet* **400**, 48–59 (2022).
2. Abuzerr, S. et al. Quantitative microbial risk assessment to estimate annual infection risk and disease burden attributable to *Escherichia coli* O157:H7 in drinking water in the Gaza Strip: a prospective study. *Lancet* **399**, S4 (2022).
3. Tao, T. & Xin, K. Public health: a sustainable plan for China's drinking water. *Nature* **511**, 527–528 (2014).
4. Nadimpalli, M. L. et al. Urban informal settlements as hotspots of antimicrobial resistance and the need to curb environmental transmission. *Nat. Microbiol.* **5**, 787–795 (2020).
5. Ling, F., Whitaker, R., LeChevallier, M. W. & Liu, W. T. Drinking water microbiome assembly induced by water stagnation. *ISME J.* **12**, 1520–1531 (2018).
6. Wang, P., Asare, E., Pitzer, V. E., Dubrow, R. & Chen, K. Associations between long-term drought and diarrhea among children under five in low- and middle-income countries. *Nat. Commun.* **13**, 3661 (2022).
7. Ray, I. & Smith, K. R. Towards safe drinking water and clean cooking for all. *Lancet Glob. Health* **9**, e361–e365 (2021).

8. Shannon, M. A. et al. Science and technology for water purification in the coming decades. *Nature* **452**, 301–310 (2008).
9. Sedlak, D. L. & von Gunten, U. The chlorine dilemma. *Science* **331**, 42–43 (2011).
10. Lindmark, M. et al. Passive in-line chlorination for drinking water disinfection: a critical review. *Environ. Sci. Technol.* **56**, 9164–9181 (2022).
11. Jones, C. H., Shilling, E. G., Linden, K. G. & Cook, S. M. Life cycle environmental impacts of disinfection technologies used in small drinking water systems. *Environ. Sci. Technol.* **52**, 2998–3007 (2018).
12. Dai, R. et al. Nanovehicle-assisted monomer shuttling enables highly permeable and selective nanofiltration membranes for water purification. *Nat. Water* **1**, 281–290 (2023).
13. Hodges, B. C., Cates, E. L. & Kim, J. H. Challenges and prospects of advanced oxidation water treatment processes using catalytic nanomaterials. *Nat. Nanotechnol.* **13**, 642–650 (2018).
14. Alvarez, P. J., Chan, C. K., Elimelech, M., Halas, N. J. & Villagrán, D. Emerging opportunities for nanotechnology to enhance water security. *Nat. Nanotechnol.* **13**, 634–641 (2018).
15. Wu, T. et al. Solar-driven efficient heterogeneous subminute water disinfection nanosystem assembled with fingerprint MoS_2. *Nat. Water* **1**, 462–470 (2023).
16. Huo, Z. Y., Du, Y., Chen, Z., Wu, Y. H. & Hu, H. Y. Evaluation and prospects of nanomaterial-enabled innovative processes and devices for water disinfection: a state-of-the-art review. *Water Res.* **173**, 115581 (2020).
17. Wang, Y. et al. Ultrasonic activation of inert poly(tetrafluoroethylene) enables piezocatalytic generation of reactive oxygen species. *Nat. Commun.* **12**, 3508 (2021).
18. Sharma, M. K. et al. Emergence of non-photoresponsive catalytic techniques for environmental remediation and energy generation. *Chem. Asian J.* **18**, e202300090 (2023).
19. Lin, Y.-J. et al. Thermocatalytic hydrogen peroxide generation and environmental disinfection by Bi_2Te_3 nanoplates. *Nat. Commun.* **12**, 180 (2021).
20. Hand, S. & Cusick, R. D. Electrochemical disinfection in water and wastewater treatment: identifying impacts of water quality and operating conditions on performance. *Environ. Sci. Technol.* **55**, 3470–3482 (2021).
21. Kotnik, T. et al. Electroporation-based applications in biotechnology. *Trends Biotechnol.* **33**, 480–488 (2015).
22. Wang, T. & Xie, X. Nanosecond bacteria inactivation realized by locally enhanced electric field treatment. *Nat. Water* **1**, 104–112 (2023).
23. Schoen, D. T. et al. High speed water sterilization using one-dimensional nanostructures. *Nano Lett.* **10**, 3628–3632 (2010).
24. Zhou, J., Wang, T. & Xie, X. Locally enhanced electric field treatment (LEEFT) promotes the performance of ozonation for bacteria inactivation by disrupting the cell membrane. *Environ. Sci. Technol.* **54**, 14017–14025 (2020).
25. Huo, Z. Y. et al. Triboelectrification induced self-powered microbial disinfection using nanowire-enhanced localized electric field. *Nat. Commun.* **12**, 3693 (2021).
26. Huo, Z. Y. et al. Synergistic nanowire-enhanced electroporation and electrochlorination for highly efficient water disinfection. *Environ. Sci. Technol.* **56**, 10925–10934 (2022).
27. Liu, C. et al. Conducting nanosponge electroporation for affordable and high-efficiency disinfection of bacteria and viruses in water. *Nano Lett.* **13**, 4288–4293 (2013).
28. Huo, Z. Y. et al. Microbial disinfection with supercoiling capacitive triboelectric nanogenerator. *Adv. Energy Mater.* **12**, 2103680 (2022).
29. Liu, C. et al. Static electricity powered copper oxide nanowire microbicidal electroporation for water disinfection. *Nano Lett.* **14**, 5603–5608 (2014).
30. Lin, S., Chen, X. & Wang, Z. L. Contact electrification at the liquid–solid interface. *Chem. Rev.* **122**, 5209–5232 (2021).
31. Wang, Z. L. & Wang, A. C. On the origin of contact-electrification. *Mater. Today* **30**, 34–51 (2019).
32. Hinchet, R. et al. Transcutaneous ultrasound energy harvesting using capacitive triboelectric technology. *Science* **365**, 491–494 (2019).
33. Ficker, T. Electrification of human body by walking. *J. Electrostat.* **64**, 10–16 (2006).
34. Kang, M. et al. Virus blocking textile for SARS-CoV-2 using human body triboelectric energy harvesting. *Cell Rep. Phys. Sci.* **3**, 100813 (2022).
35. Oh, J. et al. Dissolvable template nanoimprint lithography: a facile and versatile nanoscale replication technique. *Nano Lett.* **20**, 6989–6997 (2020).
36. Qi, D. et al. Polymeric membranes with selective solution-diffusion for intercepting volatile organic compounds during solar-driven water remediation. *Adv. Mater.* **32**, 2004401 (2020).
37. Zou, H. et al. Quantifying the triboelectric series. *Nat. Commun.* **10**, 1427 (2019).
38. Tang, W. et al. Self-powered water splitting using flowing kinetic energy. *Adv. Mater.* **27**, 272–276 (2015).
39. Liu, C. et al. Rapid water disinfection using vertically aligned MoS_2 nanofilms and visible light. *Nat. Nanotechnol.* **11**, 1098–1104 (2016).
40. Peng, L. et al. Hydrodynamic tearing of bacteria on nanotips for sustainable water disinfection. *Nat. Commun.* **14**, 5734 (2023).
41. Li, P. et al. Metal–organic frameworks with photocatalytic bactericidal activity for integrated air cleaning. *Nat. Commun.* **10**, 2177 (2019).
42. Chen, Y., Ji, Q., Zhang, G., Liu, H. & Qu, J. Synergetic lipid extraction with oxidative damage amplifies cell-membrane-destructive stresses and enables rapid sterilization. *Angew. Chem. Int. Ed.* **133**, 7823–7830 (2021).
43. Wu, H. et al. In vivo lipidomics using single-cell Raman spectroscopy. *Proc. Natl Acad. Sci. USA* **108**, 3809–3814 (2011).
44. Strahl, H. & Hamoen, L. W. Membrane potential is important for bacterial cell division. *Proc. Natl Acad. Sci. USA* **107**, 12281–12286 (2010).

Acknowledgements

This work was financially supported by the National Key R&D Program of China (grant no. 2022YFC3205400, Z.-Y.H.), the National Natural Science Foundation of China (grant no. 52200079, Z.-Y.H.), and the Basic Science Research Program (grant no. 2022R1A3B1078291, Research Leader Program, S.-W.K.) through National Research Foundation of Korea (NRF) grants funded by the Korean government (MSIT). S.-W.K. acknowledges the Yonsei Fellow Program funded by L. Y. Jae.

Author contributions

Z.-Y.H., S.-W.K. and X.W. developed the concept. Y.-J.K., Z.-Y.H. and H.D. synthesized the samples and conducted the disinfection measurements and material characterization. Y.-J.K., I.-Y.S., J.-H.H. and Y.C. fabricated the disinfection system and conducted the electrical measurements. D.-M.L. and H.Y.L. performed the electric field simulation. Y.-J.K., Z.-Y.H., X.W. and S.-W.K. analysed the data and co-wrote the paper. W.D., X.W. and Y.D. provided important experimental insights. All of the authors discussed the results and commented on the paper.

Competing interests

The authors declare no competing interests.

Additional information

Extended data is available for this paper at https://doi.org/10.1038/s44221-024-00226-5.

Supplementary information The online version contains supplementary material available at https://doi.org/10.1038/s44221-024-00226-5.

Correspondence and requests for materials should be addressed to Zheng-Yang Huo or Sang-Woo Kim.

Peer review information *Nature Water* thanks Zong-Hong Lin and the other, anonymous, reviewer(s) for their contribution to the peer review of this work.

https://doi.org/10.1038/s44221-024-00226-5

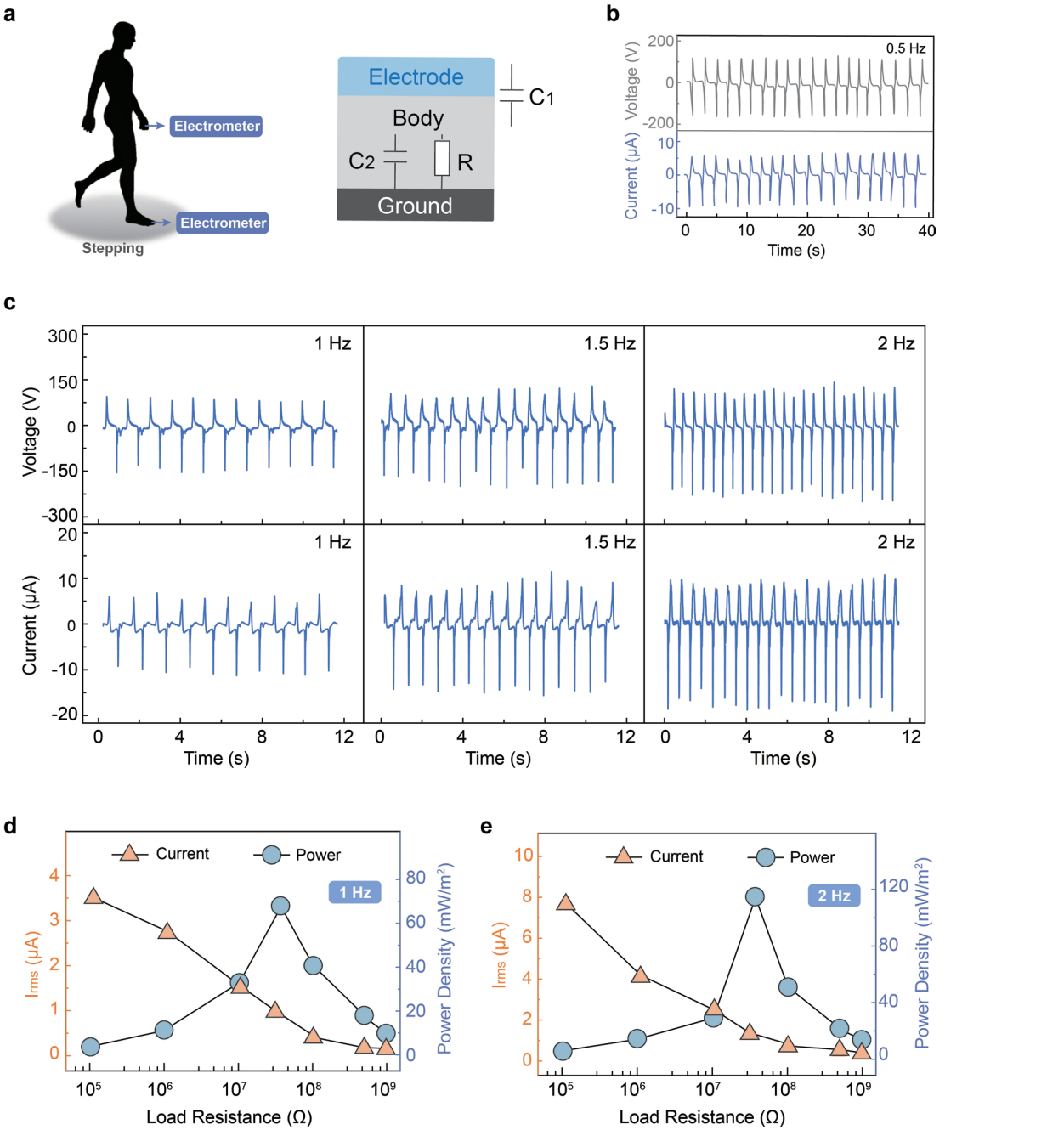

Extended Data Fig. 1 | Electrical characterization of applying the WEED method. a Schematic illustrating the method for measuring electrostatic charges induced by walking. **b** Electrical output (current and voltage) of the handheld electrode at a fixed step rate (0.5 Hz). **c** Electrical output (current and voltage) of the handheld electrode at different step rates of 1, 1.5, and 2 Hz. **d-e** Current and power density at a fixed step rate of (d) 1 and (e) 2 Hz as a function of electrical impedance (10^5 – 10^9 Ω).

https://doi.org/10.1038/s44221-024-00226-5

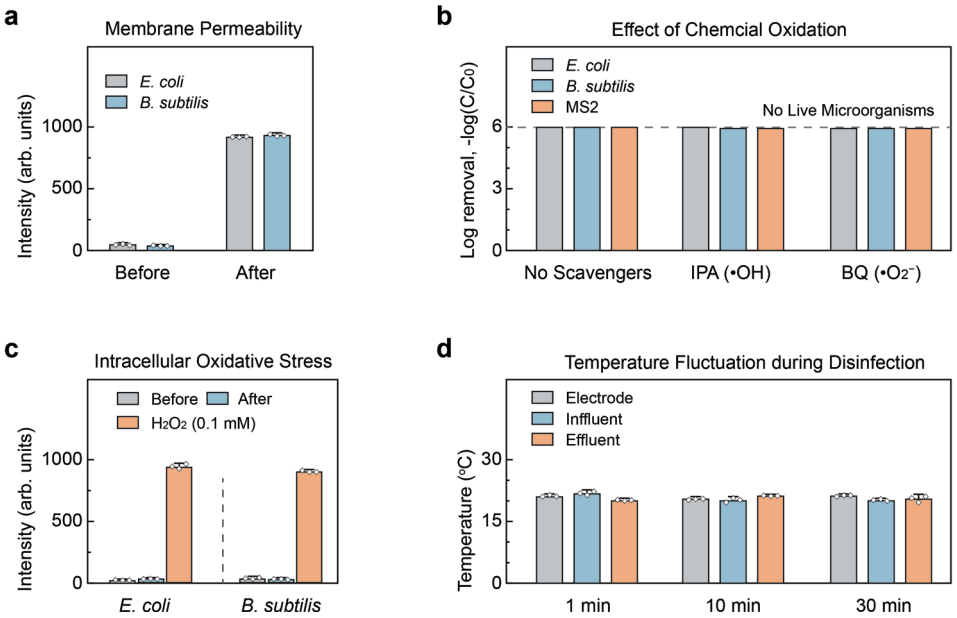

Extended Data Fig. 2 | Investigation of the disinfection mechanism of the WEED method. a Membrane permeability of bacteria before and after electroporation. **b** Effect of chemical oxidation on the disinfection performance. Scavengers of isopropanol (IPA) and benzoquinone (BQ) were used to evaluate the effects of ·OH and $\cdot O_2^-$. **c** Change in intracellular oxidative stress of bacteria caused by the potential physiological change transfer. H_2O_2 (0.1 mM) was added to the bacteria sample as the positive control group. **d** Effect of temperature on disinfection. Experiments were conducted in the disinfection demonstrator with a 10 mM PBS buffer at pH 7.0. Flow rate and step rate were fixed at 5 mL/min and 1 Hz, respectively. Dashed lines indicate that all microorganisms were inactivated (that is, live microorganisms were not detected). In a, c, and d, error bars represent the standard deviation (SD, n = 3) and data are presented as mean values + /- SD.

https://doi.org/10.1038/s44221-024-00226-5

Extended Data Fig. 3 | Photographs related to the handheld WEED bottle. **a** Photographs of the experimental setup for measuring the walking-induced electrostatic charges. **b** Photographs of the WEED bottle containing 500 mL of water. The proposed device consists of an aluminum foil (2 cm × 2 cm) on the outer surface of the bottle and four parallel nanorod-modified PPy electrodes (4 cm × 15 cm each) attached to stable acrylic supports and connected to the aluminum foil by copper wire.

nature portfolio

Corresponding author(s): Sang-Woo Kim

Last updated by author(s): Oct 21, 2023

Reporting Summary

Nature Portfolio wishes to improve the reproducibility of the work that we publish. This form provides structure for consistency and transparency in reporting. For further information on Nature Portfolio policies, see our Editorial Policies and the Editorial Policy Checklist.

Statistics

For all statistical analyses, confirm that the following items are present in the figure legend, table legend, main text, or Methods section.

n/a	Confirmed	
☐	☒	The exact sample size (*n*) for each experimental group/condition, given as a discrete number and unit of measurement
☐	☒	A statement on whether measurements were taken from distinct samples or whether the same sample was measured repeatedly
☐	☒	The statistical test(s) used AND whether they are one- or two-sided *Only common tests should be described solely by name; describe more complex techniques in the Methods section.*
☒	☐	A description of all covariates tested
☒	☐	A description of any assumptions or corrections, such as tests of normality and adjustment for multiple comparisons
☐	☒	A full description of the statistical parameters including central tendency (e.g. means) or other basic estimates (e.g. regression coefficient) AND variation (e.g. standard deviation) or associated estimates of uncertainty (e.g. confidence intervals)
☐	☒	For null hypothesis testing, the test statistic (e.g. *F*, *t*, *r*) with confidence intervals, effect sizes, degrees of freedom and *P* value noted *Give P values as exact values whenever suitable.*
☒	☐	For Bayesian analysis, information on the choice of priors and Markov chain Monte Carlo settings
☒	☐	For hierarchical and complex designs, identification of the appropriate level for tests and full reporting of outcomes
☒	☐	Estimates of effect sizes (e.g. Cohen's *d*, Pearson's *r*), indicating how they were calculated

Our web collection on statistics for biologists contains articles on many of the points above.

Software and code

Policy information about availability of computer code

Data collection	Electrical characterization data were collected using Tektronix Osciloscope data storage software.
Data analysis	Electrical characterization data were analyzed using OriginPro 9.0 and Microsoft Excel. Material characterization data were analyzed using OriginPro 9.0 and Microsoft Excel. Electric field simulations performed in this work were performed using COMSOL. Multiphysics (version 5.5). MD simulations in this work were performed using the GROMACS 2019.5 package. All statistical analyses were performed using Prism 9 software (version 9.5.0, GraphPad).

For manuscripts utilizing custom algorithms or software that are central to the research but not yet described in published literature, software must be made available to editors and reviewers. We strongly encourage code deposition in a community repository (e.g. GitHub). See the Nature Portfolio guidelines for submitting code & software for further information.

Data

Policy information about availability of data

All manuscripts must include a data availability statement. This statement should provide the following information, where applicable:

- Accession codes, unique identifiers, or web links for publicly available datasets
- A description of any restrictions on data availability
- For clinical datasets or third party data, please ensure that the statement adheres to our policy

The data supporting the results of this study are available in this paper and the supplementary information. Source data are provided in this paper. The data are available from the corresponding authors upon reasonable request.

Research involving human participants, their data, or biological material

Policy information about studies with human participants or human data. See also policy information about sex, gender (identity/presentation), and sexual orientation and race, ethnicity and racism.

Reporting on sex and gender	This study does not involve human participants.
Reporting on race, ethnicity, or other socially relevant groupings	n/a
Population characteristics	n/a
Recruitment	n/a
Ethics oversight	n/a

Note that full information on the approval of the study protocol must also be provided in the manuscript.

Field-specific reporting

Please select the one below that is the best fit for your research. If you are not sure, read the appropriate sections before making your selection.

☒ Life sciences ☐ Behavioural & social sciences ☐ Ecological, evolutionary & environmental sciences

For a reference copy of the document with all sections, see nature.com/documents/nr-reporting-summary-flat.pdf

Life sciences study design

All studies must disclose on these points even when the disclosure is negative.

Sample size	Sample size was not predetermined, but was evaluated based on the number of biological and technical replicates needed to provide adequate power for the study. We aimed to include at least 3 biological replicates, each with multiple technical replicates.
Data exclusions	No data were excluded from the analyses.
Replication	The experimental results presented in this paper have been reliably reproduced.
Randomization	Experimental subjects were randomly selected.
Blinding	This study did not need any blinding study

Reporting for specific materials, systems and methods

We require information from authors about some types of materials, experimental systems and methods used in many studies. Here, indicate whether each material, system or method listed is relevant to your study. If you are not sure if a list item applies to your research, read the appropriate section before selecting a response.

Materials & experimental systems

n/a	Involved in the study
☒	☐ Antibodies
☒	☐ Eukaryotic cell lines
☒	☐ Palaeontology and archaeology
☐	☒ Animals and other organisms
☒	☐ Clinical data
☒	☐ Dual use research of concern
☒	☐ Plants

Methods

n/a	Involved in the study
☒	☐ ChIP-seq
☒	☐ Flow cytometry
☒	☐ MRI-based neuroimaging

Animals and other research organisms

Policy information about studies involving animals; ARRIVE guidelines recommended for reporting animal research, and Sex and Gender in Research

Laboratory animals	Bacteria (E. coli: ATCC 1559 and B.subtilis: ATCC 23857 and viruses, bacteriophage MS2 ATCC 15597-B1) were used in this work.
Wild animals	The study did not involve wild animals.
Reporting on sex	The study did not involve reporting on sex.
Field-collected samples	The study did not involve field-collected samples
Ethics oversight	The number of bacteria or the number of viruses was measured by the standard spread plating method or the double agar layer method, as clearly stated and cited in the manuscript.

Note that full information on the approval of the study protocol must also be provided in the manuscript.

Plants

Seed stocks	The study did not involve seed stocks.
Novel plant genotypes	The study did not involve plant genotypes.
Authentication	n/a